A drying model for thermally large biomass particle pyrolysis

Li, Xiyan; Yin, Chungen

Published in:
Energy Procedia

DOI (link to publication from Publisher):
10.1016/j.egypro.2019.01.322

Publication date:
2019

Document Version
Version created as part of publication process; publisher's layout; not normally made publicly available

Available online at www.sciencedirect.com

ScienceDirect

Energy Procedia 00 (2018) 000–000

Energy Procedia

www.elsevier.com/locate/procedia

10th International Conference on Applied Energy (ICAE2018), 22-25 August 2018, Hong Kong, China

A drying model for large biomass particle pyrolysis using finite volume method

Xiyan Li*, Chungen Yin

Department of Energy Technology, Aalborg University, Aalborg, 9200, Denmark

Abstract

Biomass drying has always been a big issue in biomass thermal treatment. Especially in pyrolysis, combustion and gasification, water evaporation is a necessary step before other reactions can take place. This paper presents a detailed drying model using finite volume method for single poplar particle pyrolysis under nitrogen. In this model, transport equations derived from CFD code is applied to solve pressure, temperature and species behavior. Two different water contents found from literature are applied to test the model. The result shows that this model can predict water behavior during biomass drying process of pyrolysis.

Selection and peer-review under responsibility of the scientific committee of the 10th International Conference on Applied Energy (ICAE2018).

Keywords: Pyrolysis; Biomass; FVM; Drying;

Nomenclature

A	The surface area [m^2]
A_{evp}	Pre-exponential factor of water evaporation [s^{-1}]
E_{evp}	Activation energy of water evaporation, [J/Kmol].
$C_{P,S}$	Specific heat [J/(kg·K)]
$d_{pore,hydraulic}$	Hydraulic pore diameter [m]
$D_{eff,fw}$	Free water effective mass diffusivity [m^2/s]
F_{heat}	Assumed as the sum of radiation heat and convection heat transfer. [J/(kg)]

* Corresponding author. Tel.: +45_2070_3591; fax: +45_9940_3820
E-mail address: xli@et.aau.dk

h_T	Heat transfer coefficient [W/(m^2·K)]
h_M	Mass transfer coefficient [m/s]
$h_{m,pore}$	The mass transfer coefficient of vapor in the pore [m/s]
K_B	The thermal conductivity [W/(m·K)]
k_{H_2O}	Reaction rate constant [s^{-1}]
Nu	Nusselt number
Pr	Prandtl number
R_g	Universal gas constant [J/(mol·K)]
r_i	Reaction rate [J/(mol·K)]
r_{H_2O}	The volumetric vaporization rate [kg/(m^3·K)]
Sc	Schmidt number
Sh	Sherwood number
S_T	Source term in energy equation [W/m^3]
S_a	The specific area of the wood particle [m^2/m^3]
T_{ini}	Initial temperature [K]
T_∞	Ambient gas temperature [K]
T_S	Particle surface temperature [K]
$T_{j,S}$	Particle surface temperature for species j [K]
T_C	Particle center temperature [K]
T_{evap}	Defined as evaporation point of liquid water [K]
Y_{vap}	The percentage of vapor within all the species,
$Y_{j,ref}$	Reference mass fraction of species *j* in the gas film around the particle
$Y_{j,s}$	Mass fraction of species *j* at particle surface
$Y_{j,\infty}$	Mass fraction of species *j* in the ambient gas
ρ_g	Gas density [kg/m^3]
ρ_g^{sat}	The saturated vapor density [kg/m^3]
ρ_{fw}^0	The initial free water density [kg/m^3]
ρ_{fw}	The free water density at the present time [kg/m^3]
$\dot{w}_k$	Reaction rate
λ	The average conductivity of all the gases in the film [W/(m·K)]
ε	Porosity
μ	Dynamic viscosity [kg/(m·s)]
σ	Boltzmann radiation constant, 5.86×10^{-8} (W/m^2K^4)
g	Gas
l	Liquid
s	Solid

1. Introduction

Drying, as the first step of biomass gasification and pyrolysis, plays an important role in the whole process, not only for preheating, but also for the stability of industrial production. Many researchers have studied the drying technology for biomass, from lab-scale to industrial scale [1][2][3][4]. The particle size studied in literature can be as small as a pulverized particles, as well as a large piece of wood, usually around 1mm to 10 mm in diameter [5]. The drying media can be superheated steam or flue gas from biomass residues or even air or nitrogen [6]. A raw material as received usually has water content up to 40% to 50%. After drying, the water content can be 6% to 8%, which is suitable for industrial use [7].

The moisture exists in biomass in three forms: in pore and capillary as vapor or as liquid water and in fiber as bound water [3]. Normally, there is a circumscription known as Fiber saturation point (FSP) that defines the bound water and the free water. Babiak and Kudela [8] studied the definition of FSP. FSP can be 30% of dry biomass weight [9].

There are three commonly used drying models in literature, the thermal model, the kinetic rate drying model and the equilibrium model. The equilibrium model is usually used in low temperature drying, and is numerically unstable for high temperature drying [3]. The thermal model is the most commonly used model, and has been used in literature both in particle pyrolysis [10] and packed be pyrolysis [5][11]. The kinetic rate model is commonly used for bound water evaporation [12][13]. Below is a description of these three models.

Equilibrium model has the following expression. For thermal model, the expression is shown as eq. (4). For the kinetic rate model, the water evaporation is treated as a chemical reaction; hence, Arrhenius expression can be used to describe the behavior of reaction rate. The expression is shown in eq. (5).

$$H_2O(l) \xrightarrow{yields} H_2O(g) \tag{1}$$

$$r_{H_2O} = s_a(\rho_{fw}/\rho_{fw}^0)h_{m,pore}(\rho_\vartheta^{sat} - \rho_g Y_{vap}) \tag{2}$$

$$h_{m,pore} = 3.66\frac{D_{eff,fw}}{d_{pore,hydraulic}} \tag{3}$$

$$r_{H_2O} = \begin{cases} 0, & T < T_{evap} \\ \frac{F_{heat}}{\Delta h_{evap}}, & T > T_{evap} \end{cases} \tag{4}$$

$$F_{heat} = S_a\,(h_T(T_j - T_{ini}) + \varepsilon\sigma(T_j{}^4 - T_{ini}^4)) \tag{5}$$

$$r_{H_2O} = A_{evp}exp\left(-\frac{E_{evp}}{RT}\right) \tag{6}$$

Haberle et al [3] summarize the kinetic data from literature, as shown in Table1 .

Table 1 Kinetic data for water evaporation

Pre-exponential factor (s-1)	Activation energy (J Kmol-1)	Ref.
5.13×10^{10}	8.8×10^7	[12][14]
5.13×10^6	$24/120 \times 10^6$	[15]
5.60×10^8	8.8×10^7	[16]
5.13×10^6	8.8×10^7	[17]

Table 2 Proximate and ultimate analysis

Fixed carbon	9.5%
Moisture	6% and 40%
Ash	0.5%
Volatile	90%
C(DB)	48.1%
H(DB)	5.77%
O(DB)	45.53%
Others	
LHV(6% moisture)	17.05 MJ/kg
density	540kg/m3

In this work, all the three models are tested. After each time step, the local temperature will be updated at the locations where the thermal model for free water and kinetic model for bound water is active or being used. To make a comparison, a thermal model is also used for bound water and a kinetic model is used for free water, too. The simulation results shows using equilibrium model under high temperature can cause numerical instability, which is also concluded by Haberle et al[3]. Therefore, the equilibrium model is only used for free water under 100 ℃. Choosing a thermal model or choosing a kinetic model does not affect the whole pyrolysis process, although a kinetic model is preferred for bound water.

2. Model description

In order to study the drying issue of a single biomass pellet. A poplar tree particle sample is chosen from the literature [12][18] to study here, partly because the experimental data is easy to find in the literature to do model validation, partly because different water content of poplar wood particle under pyrolysis can be found in the literature. The poplar wood particle properties can be found in Table 2. The moisture here is treated as 6% and 40% the mass fraction of dry biomass. The reaction is operated under nitrogen pyrolysis and with the wall temperature of 1273K and gas flow temperature of 1050K.

A CFD code based on C++ has been generated for this model, where a finite volume method was used to solve the transport equations numerically. The convective terms are discretized by central differencing scheme, and the time step is set to 0.01s, the temporal scheme used here is implicit scheme. The meshing is along the radial direction, in which 60 grids were made. The proximate analysis and ultimate analysis, as well as density and lower heating value is given in Table 2, which is also used for validation of Lu et al's model [12] by Mehrabian et al [18]. The model assumes that the biomass particle is isotropic and near-sphere.

For wood pyrolysis, there are many kinetic models. The most commonly used ones assume a set of heat of reactions for different reactions. After that the heat of reactions are used in temperature calculations. In this work, a lower heating value (LHV) or a higher heating value (HHV) is found for the specific wood used in the pyrolysis. Therefore, the formation enthalpy of volatile can be calculated. In this work, the molecular formula of the volatile is calculated as $CH_{2.1348}O_{0.9851}$, with a molecular weight of 30.13 kg/Kmol and the formation enthalpy of $-7926\mathrm{kJ/kg}$. Assuming volatile will crack into real species: CO, CO2, H2, CH4.

Energy equation is expressed as eq. (7), while the source term can be found in eq. (6).

$$\frac{\partial(\varepsilon\rho_g C_{pg}T+\rho_s C_{ps}T)}{\partial t}+\frac{\partial(\varepsilon\rho_g u C_{pg}T_g)}{\partial r}=\frac{\partial}{\partial r}\left(k_{eff}\frac{\partial T}{\partial r}\right)+S_T \tag{7}$$

$$S_T=-\sum_{k=1}^{N}\Delta h_{f,k}^0\dot{w}_k-\sum_{k=1}^{N}\Delta h_{f,k}\dot{w}_k \tag{8}$$

S_T is the source term of energy equation and consists of a sum of formation enthalpy of each species and a sum of sensible enthalpy of each species. In this paper, whenever the source term model for water is changed, the corresponding source term in the energy equation is also replaced. For the boundary condition of temperature, the gradient is treated as 0 at center point. For the surface, due to the existence of radiation and convection, the boundary condition can be written as eq.(9). To calculate the heat transfer coefficient, a gas film surrounding the particle is assumed. The temperature used for gas properties in the gas film is treated as reference temperature, as defined by one-third law [19].

$$k_B A\frac{T_B-T_P}{\Delta r/2}=Ah_T\left(T_\infty-T_B\right)+A\varepsilon\sigma(T_\infty^4-T_B^4) \tag{9}$$

$$T_{ref}=T_s+1/3\left(T_\infty-T_s\right) \tag{10}$$

$$h_T=\frac{Nu\lambda}{d_p} \tag{11}$$

Nu denote Nusselt number, here it uses the Nusselt number from Lu et al[12] for a sphere particle, with the expression:

$$Nu\equiv\frac{h_T L_c}{k_g}=1.05+0.6Re^{0.65}Pr^{0.33} \tag{12}$$

The pressure is solved by Darcy law, together with continuity equation as follows:

$$\vec{u}=-\frac{\eta}{\mu}\nabla P \tag{13}$$

$$\frac{\partial(\varepsilon\rho_g)}{\partial t}+\frac{\partial(\varepsilon\rho_g u)}{\partial r}=S_g \tag{14}$$

The boundary condition for pressure in the center point is treated with a zero-gradient, and a mass flow conservation is used for the surface boundary condition.

For the gaseous species, a transport equation is expressed as eq. (15). Similar to the energy equation, the boundary condition of the gaseous species at center point is to set the gradients to zero. For the surface, the reference species of gas film is calculated by one-third law, as shown in eq. (16) (17), $S_{Y_{ig}}$ denotes the source term of each gas species, h_M denotes the mass transfer coefficient, and can be calculated by the following correlation. While the solid terms have the simple expression of eq. (19), ρ_i denotes the density of water, remaining volatile in solid by time t, ash and carbon, and s_i denotes their source term.

$$\frac{\partial(\varepsilon\rho_g Y_{ig})}{\partial t} + \frac{\partial(\varepsilon\rho_g u Y_{ig})}{\partial r} = \frac{\partial}{\partial r}\left(D_{ig}\frac{\partial(\varepsilon\rho_g Y_{ig})}{\partial r}\right) + S_{Y_{ig}} \quad (15)$$

$$Y_{j,ref} = Y_{j,s} + 1/3\left(Y_{j,\infty} - Y_{j,s}\right) \quad (16)$$

$$DA\frac{Y_B - Y_P}{\Delta x/2} = Ah_M(Y_\infty - Y_B) \quad (17)$$

$$Sh \equiv \frac{h_M L_c}{D_g} = 2.0 + 0.6Re^{1/2}Sc^{1/3} \quad (18)$$

$$\frac{\partial(\rho_i)}{\partial t} = s_i \quad (19)$$

All the reactions used in this model are listed in Table 3. A one-step global biomass decomposition model is used in this work. Thermal model and kinetic model used for moisture evaporation have already been stated in Equ. (2) to (6), the results will be discussed later in this paper. All the kinetics data used in Table 3 is shown in Table 4.

Table 4: Kinetic data used in this model

Reaction index	Pre-exponential factor(s^{-1})	Activation energy(J/Kmol)	Heat of reactions (KJ/kg)
1	3.4×10^4	6.9×10^7	-1376.09
2	-	-	-
3	5.13×10^{10}	8.8×10^7	-2440
4	0.658a	7.4831×10^7	3950
5	3.42a	1.297×10^5	-14383.33
6	3.42a	1.297×10^5	-10933.33
7	2083a	115137	1701.59
7	$10^{12.71}$	1.71×10^5	13435.94
8	2.39×10^{12}	1.702×10^8	10114.28
9	3.0×10^8	1.26×10^8	-12879,38
10	5.012×10^{11}	2.0×10^8	2233.13
11	2.75×10^9	8.4×10^7	1480

a Those units are m/s-1k-1

TABLE 3: Chemical reactions and reaction rate

Reaction index	Chemical reactions	Rate expression	Ref
1	Biomass → Volatile + Char	$r_1 = \partial\rho_{Vol}/\partial t = k_1\rho_{vol}$	[20]
2	H2O (free)→ H2O (g)	Equation (2-6)	
3	H2O(bound)→H2O (g)	Equation (2-6)	
4	C+1/2O2→CO	$r_4 = \partial C_{O_2}/\partial t = s_{a,char}[\rho_C/(\rho_C + \rho_B + \rho_A)]k_4 C_{O_2}$	[12]
5	C+CO2→2CO	$r_5 = \partial C_{CO_2}/\partial t = s_{a,char}[\rho_C/(\rho_C + \rho_B + \rho_A)]k_5 C_{CO_2}$	[12]
6	C+H2O→H2 + CO	$r_6 = \partial C_{H_2O}/\partial t = s_{a,char}[\rho_C/(\rho_C + \rho_B + \rho_A)]k_6 C_{H_2O}$	[12]
7	C+2H2→ CH4	$r_7 = \partial C_{H_2}/\partial t = s_{a,char}[\rho_C/(\rho_C + \rho_B + \rho_A)]k_7 C_{H_2}$	[21]
8	H2+1/2O2→H2O	$r_8 = \partial H_2/\partial t = k_8 C_{H_2} C_{O_2}^{0.5}$	[22]
9	CO+1/2O2→CO2	$r_9 = \partial C_{CO}/\partial t = k_9 C_{CO} C_{O_2}^{0.25} C_{H_2O}^{0.5}$	[12]
10	CH4+H2O→CO+3H2	$r_{10} = \partial C_{CH_4}/\partial t = k_{10} C_{CH_4}^{1.0} C_{H_2O}^{1.0}$	[23]
11	CH4+0.5O2→CO+2H2	$r_{11} = \partial C_{CH_4}/\partial t = k_{11} C_{CH_4}^{0.7} C_{H_2O}^{0.8}$	[23]
12	CO+H2O→CO2+H2	$r_{12} = \partial C_{CO}/\partial t = k_{12} C_{CO}^{1} C_{H_2O}^{1}$	[23]

3. Model validation and discussion

A grid independence check is made in Fig.1 A). The simulation results are based on 6% moisture content under nitrogen pyrolysis. As mentioned in introduction, 6% moisture content is far away from FSP, the reaction mechanism used in Fig1 is kinetic model. 60, 80, 100 grids along the radius were meshed, respectively. The grid independence check shows that the results from this model are independent of the meshing. Fig. 1 A) also shows three obvious pyrolysis stage as shown by arrows. It can be seen that the water vanishes around 6th or 7th second. The devolatilization stage stops after 32 seconds. The first stage is called drying stage, it stops after 6 seconds. During this stage, the free

water and some bound water release. The biomass is slightly heated. The second stage is the devolatilization stage, the pre-pyrolysis takes place from 400K to 700K with the release of light gases. The weight loss loses quickly in this stage (will be discussed in extended version), which is also a sign of gases releasing. Once the devolatilization reaction is finished, the temperature of the poplar particle goes up immediately, the pyrolysis comes to the final stage, in this stage the large molecules crack into char or noncondensable gases (will be discussed in extended version). The light gases take reactions or leave the pellet quickly. More information to show the three stages and the comparison of the mass fraction will be discussed later.

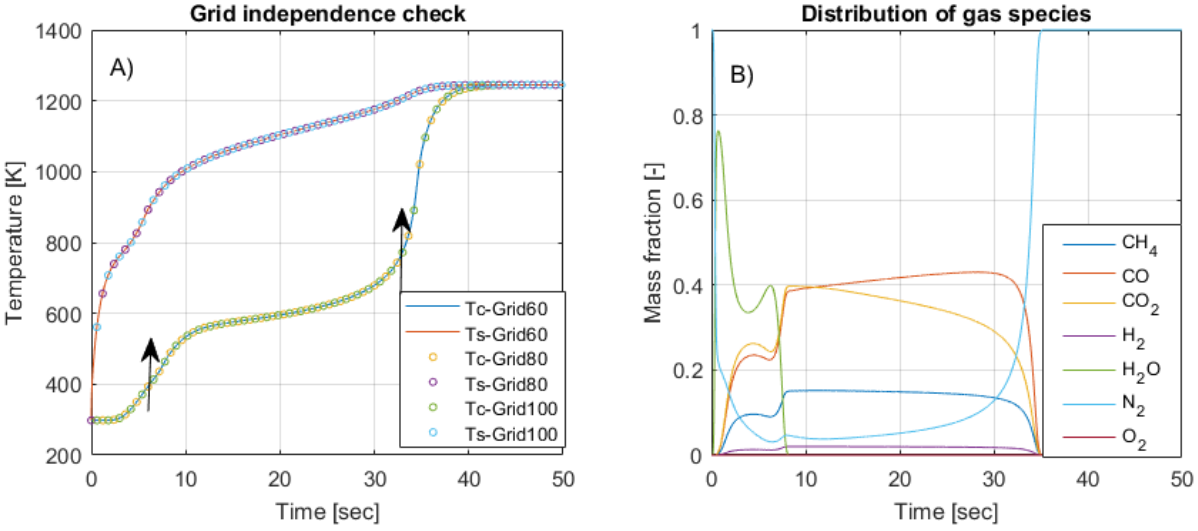

Fig 1A) Grid independence check. B) Gas species release with respect to time

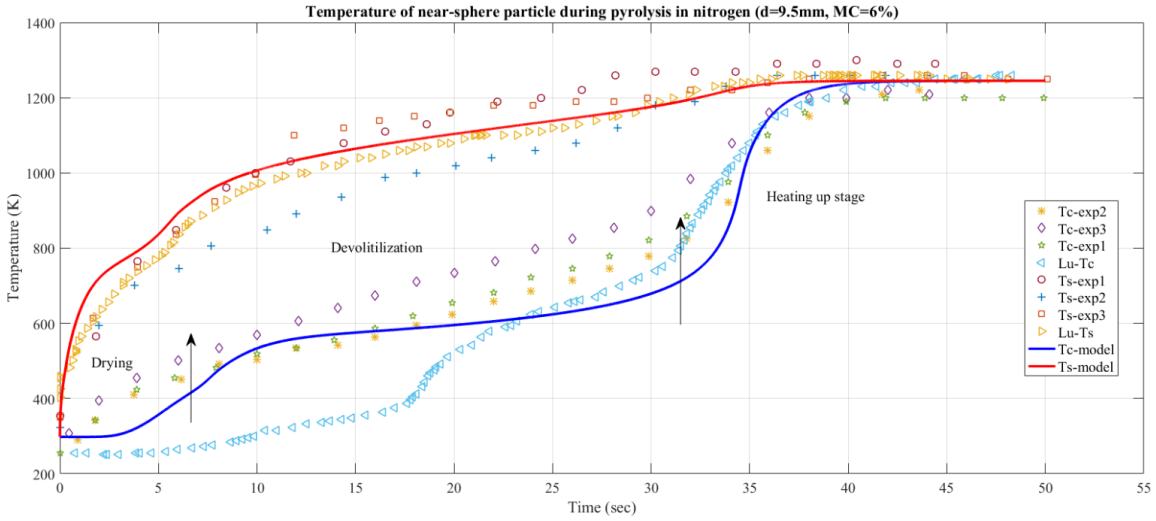

Fig. 2 Temperature profile from model and lu et al's results

Figure 1 B) shows the light gases released from the pyrolysis process at the center point of biomass pellet. It uses the same amount of moisture content as in Fig.1 A). The green line is water vapor release curve. Obviously, there are two peeks in this curve. The first one is because the fast release of free water. With the decomposition of biomass starts, the other small molecular-weight gases, like H_2, CO, CO_2, CH_4, the mass fraction of water vapor decreases. This stage is called initial stage by Basu [24], around temperature 100℃ to 300℃. The mass fraction of water goes

down because the mass fraction of other gas species come out. Another vapor peak is caused by the intermediate stage (200℃ to 600℃) [24], where the primary pyrolysis starts. This stage finished until 35th second. During pyrolysis, there is not many homogeneous reactions happening after devolitilization stage. Fig. 1A) shows the devolitilization stops around 32 seconds, after that, as shown in Fig.1 B), the mass fraction of small molecules gas species decreases and comes to zero after 35 seconds. After that, there is no other gas coming out. As a result, the third stage is mainly heating up stage caused by the heat transfer from the surrounding environment.

The model has been validated using H. Lu et al's [12] experimental results and Rath et al's results[25], separately. In both validation, the modelling results shows a nice agreement with the experiments that Lu et al and Rath et al made. In experiment that Lu et al did, a poplar biomass particle is exposed to a furnace of 1276K with the flow temperature of 1050K. The gas media is nitrogen, the water content is set to 6% for sphere pellet and 40% for cylinder pellet. Since this work focuses on simulation of a sphere pellet, 6% moisture content from Lu et al's experimental work is used for comparison here. Simulation of 40% moisture content biomass pellet under nitrogen pyrolysis will be discussed, too. The validation against experimental results from Lu et al is shown in Fig. 2.

In Fig. 2, the solid blue line is temperature for center point from simulation result that authors made, the solid red line is the temperature for surface point using the simulation that authors made. It also shows the three experimental data from Lu et al and the simulation results from Lu et al. As shown in Fig. 2, the simulation agrees with experiment data better than the modelling results that H. Lu et al show. A one-step global devolatilization model for biomass decomposition is used here. Depending on the kinetic data that is chosen, the time interval of plateau in Fig.2 between the two arrows can be different. The devolatilization model affects the devolatilization rate, as discussed by Yang et al [26]. Here a 'fast' one-step devolatilization rate by Nunn[27] and defined by Yang et al[26] is used in this model, because it shows a better simulation result for poplar wood used by Lu et al [12] and Mehrabian et al [18]. The plot of center point temperature shows clearly three stage of devolatilization, drying and heating up stage after reactions are finished.

Conclusion

A CFD model based on finite volume method was used to study the drying of a poplar particle during pyrolysis process. The model uses one-step global biomass decomposition reactions to describe the pressure, temperature and species behavior of the drying process. A validation using literature data shows good agreement with experimental results. In extended version, water behavior from using two different kind of water evaporation models has been discussed. The results show using thermal model can cause longer time of drying stage and therefore delay the following up reactions. To better balance the thermal model and kinetic model, it is suggested here when the moisture content is over FSP, both thermal and kinetic water evaporation models should be considered in the biomass pyrolysis process.

Acknowledgements

The Authors are grateful to the help from department of energy technology of Aalborg University and support from Chinese scholarship council.

References

[1] Messai S, Sghaier J, Lecomte D, Belghith A. Drying kinetics of a porous spherical particle and the inversion temperature. Dry Technol 2008;26:157–67. doi:10.1080/07373930701831127.
[2] Mezhericher M, Levy A, Borde I. The influence of thermal radiation on drying of single droplet/wet particle. Dry Technol 2008;26:78–89. doi:10.1080/07373930701781686.
[3] Haberle I, Haugen NEL, Skreiberg Ø. Drying of thermally thick wood particles: A study of the numerical efficiency, accuracy, and stability of common drying models. Energy & Fuels 2017:acs.energyfuels.7b02771. doi:10.1021/acs.energyfuels.7b02771.
[4] Rezaei H, Lim CJ, Lau A, Bi X, Sokhansanj S. Development of empirical drying correlations for ground wood chip and ground wood pellet particles. Dry Technol 2017;35:1423–32. doi:10.1080/07373937.2016.1198912.
[5] Yang YB, Sharifi VN, Swithenbank J. Effect of air flow rate and fuel moisture on the burning behaviours of biomass and simulated municipal solid wastes in packed beds. Fuel 2004;83:1553–62. doi:10.1016/j.fuel.2004.01.016.
[6] Ståhl M, Granström K, Berghel J, Renström R. Industrial processes for biomass drying and their effects on the quality properties of wood pellets. Biomass and Bioenergy 2004;27:621–8. doi:10.1016/j.biombioe.2003.08.019.

[7] Di Blasi C, Hernandez EG, Santoro A. Radiative pyrolysis of single moist wood particles. Ind Eng Chem Res 2000;39:873–82. doi:10.1021/ie990720i.
[8] Babiak M, Kúdela J. A contribution to the definition of the fiber saturation point. Wood Sci Technol 1995;29:217–26. doi:10.1007/BF00204589.
[9] Di Blasi C. Multi-phase moisture transfer in the high-temperature drying of wood particles. Chem Eng Sci 1998;53:353–66. doi:10.1016/S0009-2509(97)00197-8.
[10]Yang YB, Sharifi VN, Swithenbank J, Ma L, I L, Jones JM, et al. Combustion of a single particle of biomass. Energy 2008:306–16. doi:10.1021/ef700305r.
[11]Yang YB, Lim CN, Goodfellow J, Sharifi VN, Swithenbank J. A diffusion model for particle mixing in a packed bed of burning solids. Fuel 2005;84:213–25. doi:10.1016/j.fuel.2004.09.002.
[12]Lu H, Robert W, Peirce G, Ripa B, Baxter LL. Comprehensive study of biomass particle combustion. Energy and Fuels 2008;22:2826–39. doi:10.1021/ef800006z.
[13]Bryden KM, Hagge MJ. Modeling the combined impact of moisture and char shrinkage on the pyrolysis of a biomass particle. Fuel 2003;82:1633–44. doi:10.1016/S0016-2361(03)00108-X.
[14]Fatehi H, Bai XS. A comprehensive mathematical model for biomass combustion. Combust Sci Technol 2014;186:574–93. doi:10.1080/00102202.2014.883255.
[15]Peters B, Bruch C. Drying and pyrolysis of wood particles: experiments and simulation. Fuel Energy Abstr 2004;45:100. doi:10.1016/S0140-6701(04)93143-8.
[16]Blasi C Di, Branca C, Sparano S, Mantia B La. Drying characteristics of wood cylinders for conditions pertinent to ÿxed-bed countercurrent gasiÿcation 2003;25:45–58.
[17]Chan WCR, Kelbon M, Krieger BB. Modelling and experimental verification of physical and chemical processes during pyrolysis of a large biomass particle. Fuel 1985;64:1505–13. doi:10.1016/0016-2361(85)90364-3.
[18]Mehrabian R, Zahirovic S, Scharler R, Obernberger I, Kleditzsch S, Wirtz S, et al. A CFD model for thermal conversion of thermally thick biomass particles. Fuel Process Technol 2012;95:96–108. doi:10.1016/j.fuproc.2011.11.021.
[19]Yin C. Modelling of heating and evaporation of n-Heptane droplets: Towards a generic model for fuel droplet/particle conversion. Fuel 2015;141:64–73. doi:10.1016/j.fuel.2014.10.031.
[20]Yang YB, Yamauchi H, Nasserzadeh V, Swithenbank J. Effects of fuel devolatilisation on the combustion of wood chips and incineration of simulated municipal solid wastes in a packed bed. Fuel 2003;82:2205–21. doi:10.1016/S0016-2361(03)00145-5.
[21]Klose E, Köpsel R. Mathematical model for the gasification of coal under pressure. Fuel 1978;72:714. doi:10.1016/0016-2361(93)90662-L.
[22]Zhou H, Jensen AD, Glarborg P, Jensen PA, Kavaliauskas A. Numerical modeling of straw combustion in a fixed bed. Fuel 2005;84:389–403. doi:10.1016/j.fuel.2004.09.020.
[23]Yin C, Kær SK, Rosendahl L, Hvid SL. Co-firing straw with coal in a swirl-stabilized dual-feed burner: Modelling and experimental validation. Bioresour Technol 2010;101:4169–78. doi:10.1016/j.biortech.2010.01.018.
[24]Basu P. Biomass Gasification and Pyrolysis: Practical Design. vol. 28. 2010. doi:10.1017/CBO9781107415324.004.
[25]Rath J, Steiner G, Wolfinger MG, Staudinger G. Tar cracking from fast pyrolysis of large beech wood particles. J Anal Appl Pyrolysis 2002;62:83–92. doi:10.1016/S0165-2370(00)00215-1.
[26]Yang YB, Yamauchi H, Nasserzadeh V, Swithenbank J. Effects of fuel devolatilisation on the combustion of wood chips and incineration of simulated municipal solid wastes in a packed bed. Fuel 2003;82:2205–21. doi:10.1016/S0016-2361(03)00145-5.
[27]Nunn TR, Howard JB, Longwell JP, Peters WA. Product compositions and kinetics in the rapid pyrolysis of milled wood lignin. Ind Eng Chem Process Des Dev 1985;24:844–52. doi:10.1021/i200030a054.